

Electronic Supplementary Information (ESI)

Wastewater depollution of textile dyes and antibiotics using unmodified and copper oxide/zinc oxide nanofunctionalised graphene oxide materials

Piumie Rajapaksha^a, Rebecca Orrell-Trigg^a, Yen B. Truong^b, Daniel Cozzolino^c, Vi Khanh Truong^a, James Chapman^{a*}

^aSchool of Science, RMIT University, 124 La Trobe St, Melbourne VIC 3000, Australia.

^cCSIRO Materials Science and Engineering, Commonwealth Scientific and Industrial Research Organization (CSIRO), Clayton, Victoria 3168, Australia.

^cCentre for Nutrition and Food Sciences, The University of Queensland, St Lucia, Brisbane, QLD 4069, Australia.

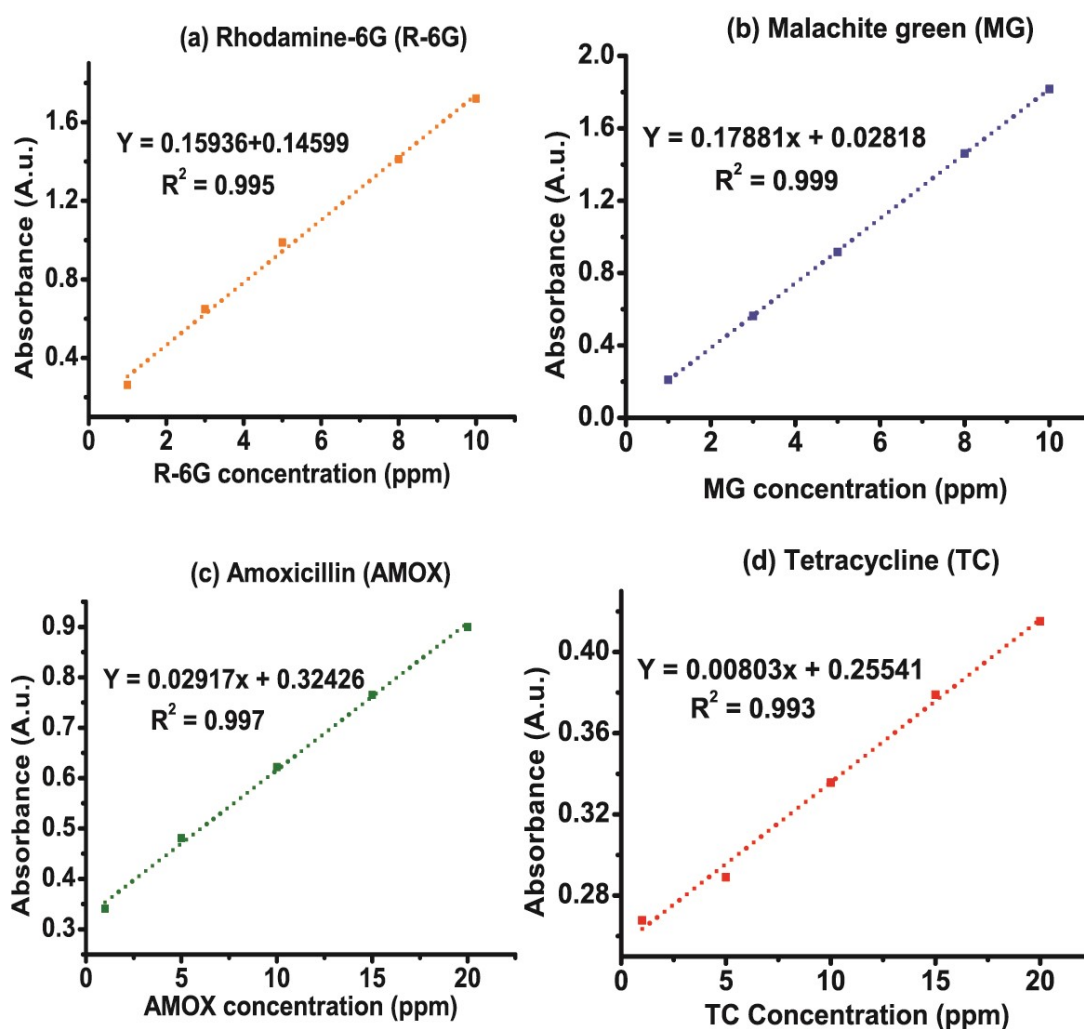


Figure S1. The calibration plots over a series of concentrations of the dyes (a) R-6G, (b) MG and antibiotics (c) AMOX and (d) TC

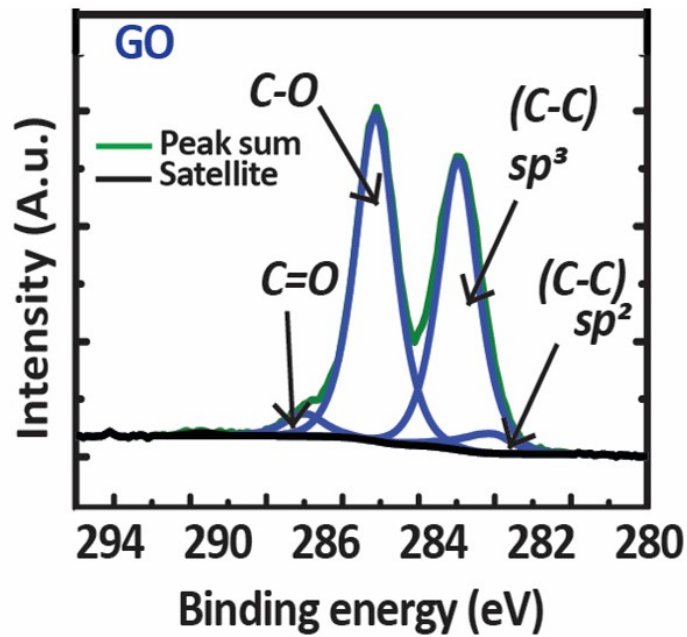


Figure S2. The deconvoluted XPS at C1s spectra of GO

The high resolution of C1s spectra was deconvoluted using CasaXPS software with a Shirley background model. The signals were received at 533 eV and 287 eV representing O1s and C1s electrons respectively, which represents C-O/C-OH and C-C bonding. The deconvoluted spectra at C1s of GO showed various oxygen functional groups. The deconvolution spectra at C1s of GO showed intensified peaks at 284 eV, 285 eV, 287 eV and 289 eV representing C-C (*sp*²), C-C (*sp*³), C-O and C=O respectively. This suggests the prevalence of oxygen functional sites that facilitates attracting the contaminant molecules during the adsorption processes.

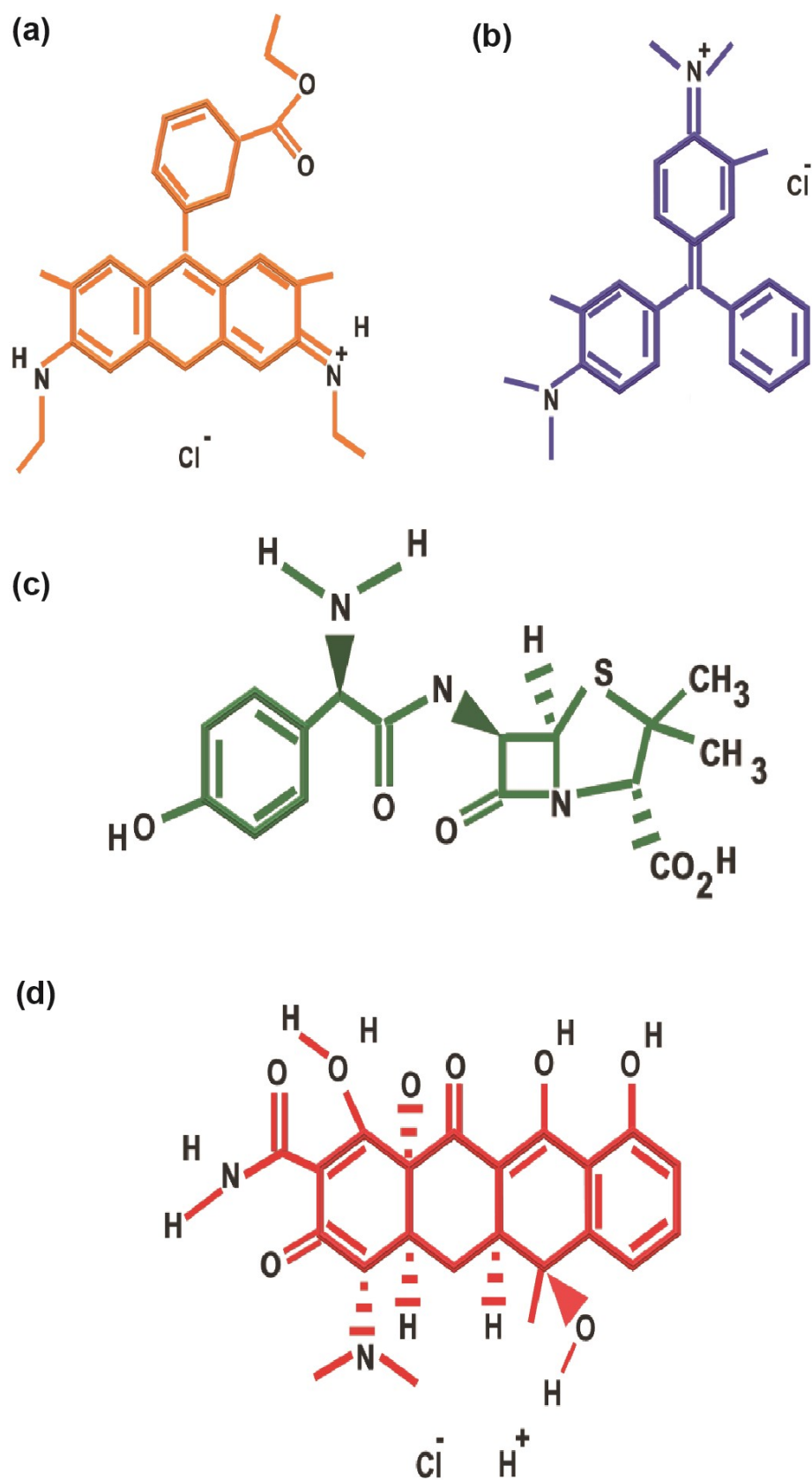


Figure S3. The molecular structures of (a) Rhodamine-6G (R-6G), (b) malachite green (MG) dyes and (c) amoxicillin (AMOX) and tetracycline (TC) antibiotics.

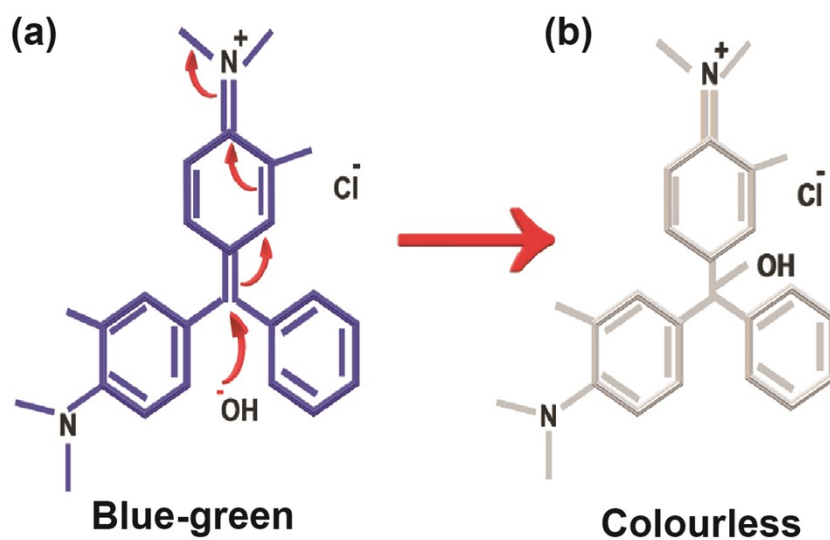


Figure S4. The schematic of showing the reaction of malachite green (MG) molecule with hydroxide ions from sodium hydroxide producing an instant colourless solution.

MG is consisted of planar ring system that gives the colour of blue-green. The hydroxide ions from sodium hydroxide attack the central C atom and therefore, the planarity is destroyed, thus the blue-green colour is disappeared giving a colourless solution.

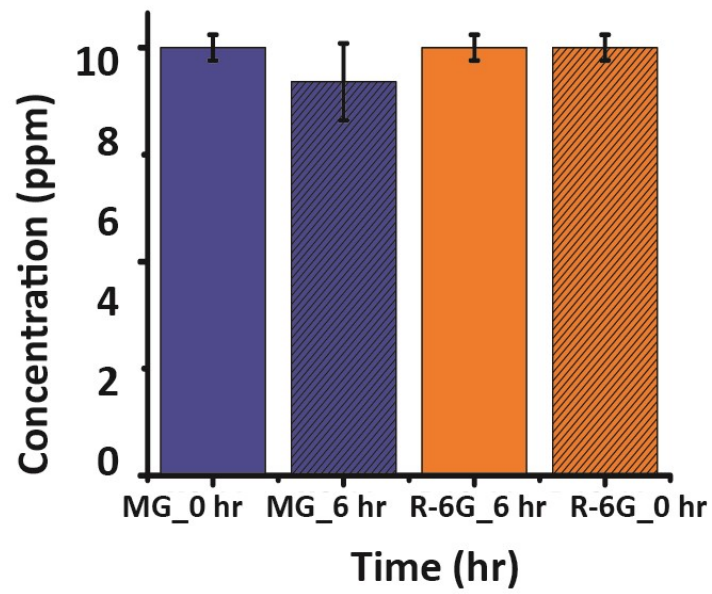


Figure S5. The column chart comparing the MG and R-6G dye concentrations under the same experimental conditions after 6 hr period of time without using the adsorbents. The R-6G concentration was not changed over the time. The MG concentration was decreased from 10 ppm to 9.2 ppm over 6 hrs, indicating 8% photo-degradation of the MG dye.

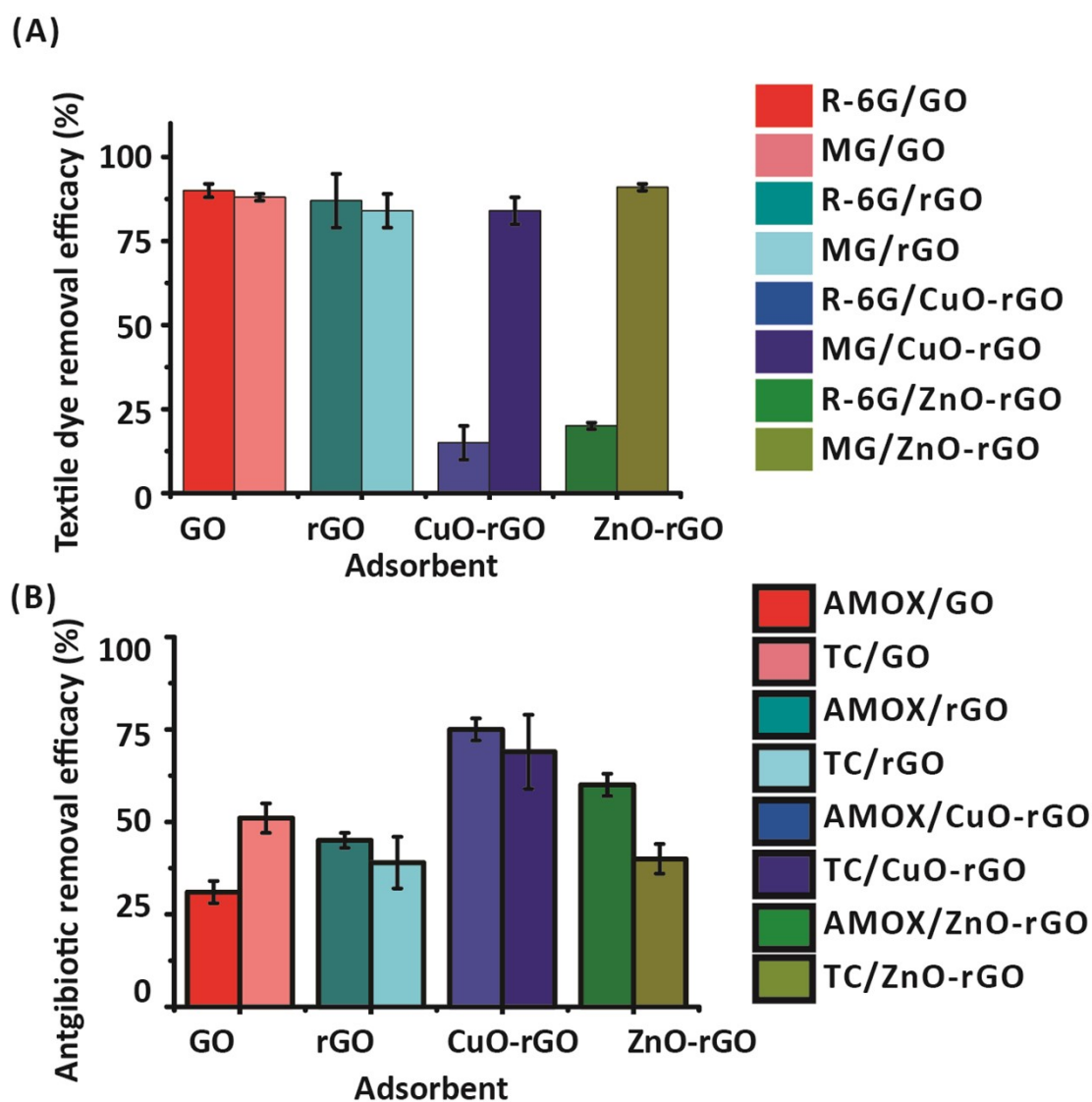


Figure S6. The column chart showing the dye removal (A) and antibiotic removal (B) efficacies using the GO, rGO, CuO-rGO and ZnO-rGO adsorbents. The rGO was an excellent adsorbent removing cationic dyes as well as GO showing 87% and 84% R-6G and MG respectively. In addition, rGO was lesser effective in removing AMOX and TC by 45% and 39%, respectively.

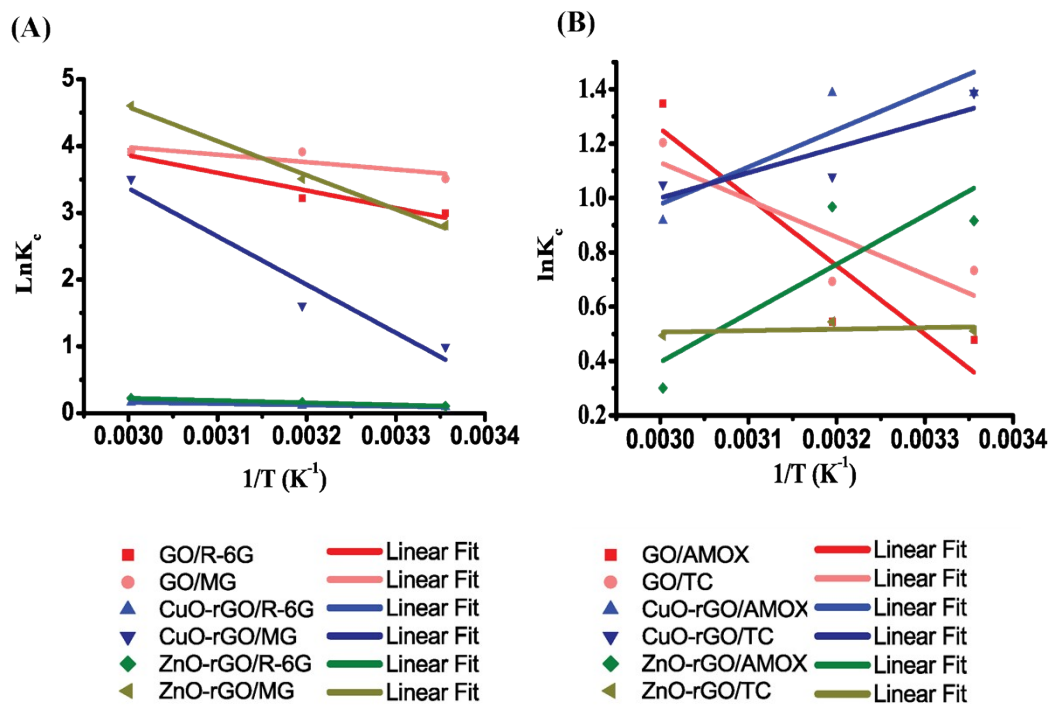


Figure S7. The linear plots of $\ln k_c$ vs $1/T$ for the (A) Dyes; R-6G, MG and (B) Antibiotics; AMOX and TC on GO, CuO-rGO and ZnO-rGO adsorbents

Table S1. The comparison of the adsorption isotherms of dye molecules onto GO in the recent studies

	Reference	Adsorbent	Dye	Q_{\max} (mg/g)	ΔG (kJ/mol)	R^2
	Current study	GO	MG	813	-10.83	0.997
			R-6G	625	-10.83	0.991
		CuO-rGO	MG	909	-9.7	0.999
		ZnO-rGO	MG	870	-12.74	0.999
1)	Araujo <i>et al.</i> , 2019 ¹	GO	Methylene blue (MB)	308.11	NA	0.96
2)	Mao <i>et al.</i> , 2020 ²	GO	MB	403.3	-46.3	0.996
		Fluorinated-GO	MB	306.5	-41.9	0.989
		Interconnected-rGO	MB	106.0	-34.1	0.984
3)	Arias <i>et al.</i> , 2020 ³	r-GO	MB	121.95	-25.16	0.984
4)	Du <i>et al.</i> , 2016 ⁴	Graphene-Melamine-Sponge	MB	286.5	NA	0.994
5)	Liu <i>et al.</i> , 2015 ⁵	Magnetite/r-GO (MRGO)	MB	144.9	-12.47	0.9959
6)	Wang <i>et al.</i> , 2015 ⁶	Magnetic β -cyclodextrin-graphene oxide nanocomposites (Fe ₃ O ₄ / β -CD/GO)	MB	740.74	-2.021	0.9945
7)	Gupta <i>et al.</i> , 2017 ⁷	r-GO	R-6G	476.2	-14.573	0.997
8)	Gao <i>et al.</i> , 2019 ⁸	Magnetic GO decorated with persimmon tannins	MG	560.58	-11.62	0.999
9)	Liu <i>et al.</i> , 2012 ⁹	3D-GO	MB	397	47.7	0.999
			MV	467	68.2	0.999
10)	Sabna <i>et al.</i> , 2018 ¹⁰	GO	Crystal violet (CV)	207.4	NA	0.956
			Methyl orange (MO)	37.2	NA	0.998

Table 2. The comparison of the adsorption isotherms of antibiotic molecules onto GO in the recent studies

	Reference	Adsorbent	Antibiotic	q_{\max} (mg/g)	ΔG (kJ/mol)	R^2
	Current study	GO	AMOX	239	-3.72	0.985
			TC	281	-3.33	0.986
		CuO-rGO	AMOX	404	-3.60	0.999
			TC	552	-2.80	0.999
		ZnO-rGO	AMOX	241	-2.51	0.995
			TC	48	-1.41	0.961
1)	Salihi <i>et al.</i> , 2021 ¹¹	GO	Trimethoprim (TMP)	204.08	NA	0.952
			Isoniazid (INH)	13.89	NA	0.930
2)	Gao <i>et al.</i> , 2012 ¹²	GO	TC	313.480	NA	0.992
			Oxytetracycline	212.314	NA	0.864
			Doxycycline	398.406	NA	0.950
3)	Chaba <i>et al.</i> , 2019 ¹³	Zinc oxide coated carbon nanofiber composite	AMOX	156	NA	0.9988
4)	Zhong <i>et al.</i> , 2020 ¹⁴	Petal-Like Magnetic-rGO (MrGO)	Sulfadiazine	6.27 $\mu\text{g}/\text{mg}$	NA	0.987
		rGO	Sulfadiazine	7.24	NA	0.993
5)	Huizar-Félix <i>et al.</i> , 2019 ¹⁵	rGO decorated with $\alpha\text{-Fe}_2\text{O}_3$ Nanoparticles	TC	18.47	NA	0.965
		rGO	TC	44.23	NA	0.975
6)	Bao <i>et al.</i> , 2018 ¹⁶	Magnetic $\text{MnFe}_2\text{O}_4/\text{rGO}$ nanocomposite	TC	41	NA	0.9723
7)	Ghadim <i>et al.</i> , 2013 ¹⁷	GO	TC	323	-2.0068	0.997
8)	Zhu <i>et al.</i> , 2017 ¹⁸	GO/calcium alginate (GO/CA) composite	TC	131.6	NA	0.9938
9)	Ghadiri <i>et al.</i> , 2020 ¹⁹	Amine-functionalized bio-graphene (AFBG)	Ciprofloxacin (CIP)	172.6	-7.5	0.99
10)	Ma <i>et al.</i> , 2017 ²⁰	GO	TC	272.70	NA	0.89
		KOH-GO	TC	532.59	NA	0.84

References

1. C. M. Bezerra de Araujo, G. Filipe Oliveira do Nascimento, G. Rodrigues Bezerra da Costa, K. Santos da Silva, A. M. Salgueiro Baptisttella, M. Gomes Ghislandi and M. Alves da Motta Sobrinho, *Chemical Engineering Communications*, 2019, **206**, 1375-1387.
2. B. Mao, B. Sidhureddy, A. R. Thirupathi, P. C. Wood and A. Chen, *New Journal of Chemistry*, 2020, **44**, 4519-4528.
3. F. Arias Arias, M. Guevara, T. Tene, P. Angamarca, R. Molina, A. Valarezo, O. Salguero, C. Vacacela Gomez, M. Arias and L. S. Caputi, *Nanomaterials*, 2020, **10**, 681.
4. Q. Du, Y. Zhou, X. Pan, J. Zhang, Q. Zhuo, S. Chen, G. Chen, T. Liu, F. Xu and C. Yan, *RSC advances*, 2016, **6**, 54589-54596.
5. G. Liu, N. Wang, J. Zhou, A. Wang, J. Wang, R. Jin and H. Lv, *RSC advances*, 2015, **5**, 95857-95865.
6. C. Wang, B. Li, W. Niu, S. Hong, B. Saif, S. Wang, C. Dong and S. Shuang, *RSC advances*, 2015, **5**, 89299-89308.
7. K. Gupta and O. P. Khatri, *Journal of colloid and interface science*, 2017, **501**, 11-21.
8. M. Gao, Z. Wang, C. Yang, J. Ning, Z. Zhou and G. Li, *Colloids and Surfaces A: Physicochemical and Engineering Aspects*, 2019, **566**, 48-57.
9. F. Liu, S. Chung, G. Oh and T. S. Seo, *ACS applied materials & interfaces*, 2012, **4**, 922-927.
10. V. Sabna, S. G. Thampi and S. Chandrakaran, *Water Science and Technology*, 2018, **78**, 732-742.
11. E. Çalışkan Salihi, J. Wang, G. Kabacaoğlu, S. Kirkulak and L. Šiller, *Separation Science and Technology*, 2021, **56**, 453-461.
12. Y. Gao, Y. Li, L. Zhang, H. Huang, J. Hu, S. M. Shah and X. Su, *Journal of colloid and interface science*, 2012, **368**, 540-546.
13. J. M. Chaba and P. N. Nomngongo, *Emerging Contaminants*, 2019, **5**, 143-149.
14. J. Zhong, Y. Feng, J.-L. Li, B. Yang and G.-G. Ying, *Water*, 2020, **12**, 1933.
15. A. M. Huízar-Félix, C. Aguilar-Flores, A. Martínez-de-la Cruz, J. M. Barandiarán, S. Sepúlveda-Guzmán and R. Cruz-Silva, *Nanomaterials*, 2019, **9**, 313.
16. J. Bao, Y. Zhu, S. Yuan, F. Wang, H. Tang, Z. Bao, H. Zhou and Y. Chen, *Nanoscale research letters*, 2018, **13**, 1-8.
17. E. E. Ghadim, F. Manouchehri, G. Soleimani, H. Hosseini, S. Kimiagar and S. Nafisi, *PLoS One*, 2013, **8**, e79254.
18. H. Zhu, T. Chen, J. Liu and D. Li, *RSC advances*, 2018, **8**, 2616-2621.
19. S. K. Ghadiri, H. Alidadi, N. Tavakkoli Nezhad, A. Javid, A. Roudbari, S. S. Talebi, A. A. Mohammadi, M. Shams and S. Rezaia, *Plos one*, 2020, **15**, e0231045.
20. J. Ma, Y. Sun and F. Yu, *Royal Society open science*, 2017, **4**, 170731.